ARTICLE

Shock Tube Measurement of Ethylene Ignition Delay Time and Molecular Collision Theory Analysis

Xiao-he Xiong, Yan-jun Ding, Shuo Shi, Zhi-min Peng*

State Key Lab of Power Systems, Department of Thermal Engineering, Tsinghua University, Beijing 100084, China

(Dated: Received on May 11, 2016; Accepted on August 24, 2016)

In this study, 75% and 96% argon diluent conditions were selected to determine the ignition delay time of stoichiometric mixture of $C_2H_4/O_2/Ar$ within a range of pressures (1.3−3.0 atm) and temperatures (1092−1743 K). Results showed a logarithmic linear relationship of the ignition delay time with the reciprocal of temperatures. Under both two diluent conditions, ignition delay time decreased with increased temperature. By multiple linear regression analysis, the ignition delay correlation was deduced. According to this correlation, the calculated ignition delay time in 96% diluent was found to be nearly five times that in 75% diluent. To explain this discrepancy, the hard-sphere collision theory was adopted, and the collision numbers of ethylene to oxygen were calculated. The total collision numbers of ethylene to oxygen were 5.99×10^{30} $s^{-1}cm^{-3}$ in 75% diluent and 1.53×10^{29} $s^{-1}cm^{-3}$ in 96% diluent (about 40 times that in 75% diluent). According to the discrepancy between ignition delay time and collision numbers, *viz.* 5 times corresponds to 40 times, the steric factor can be estimated.

Key words: Shock tube, Ethylene, Ignition delay, Molecule collision

I. INTRODUCTION

Ethylene is a significant product during the large hydrocarbon molecule pyrolysis and its reaction mechanism attracts considerable attention. To a thermal chemist, shock tube [1] is an effective study tool as the test gas volume can be heated near-instantaneously with a spatially uniform distribution [2]. To investigate the combustion reactions, the ignition delay time of hydrocarbon fuels is measured under different temperatures [3], pressures [4], and equivalent ratios [5] using a shock tube. Combined with these experimental results, the mainstream mechanism models (*e.g.*, USC II [6], GRI 3.0 [7], and NUI C4 [8]) can be adopted to analyze the oxidation details by certain methods including sensitivity analysis [9], reaction path analysis [10], *etc.* Although the ignition delay time can be calculated by running these models, the cost is long calculating time needed (especially in those complex mechanisms). Moreover, the prediction performance of these mechanism models is not good under special conditions, such as low temperature or high pressure area in certain reactions. For example, Pang *et al.* [11] studied the combustion reaction of $H_2/O_2/Ar$ mixtures and found that the prediction results of the GRI 3.0 mechanism were far larger than the experimental results. In addition, these mechanisms also do not agree well with certain type of fuels. Zhang *et al.* [12] compared the reaction results of C1−C4 alkanes using USC II and NUI C4 mechanisms and found that USC II is under-prediction for ethane. Zhang *et al.* [12] attributed this inconsistency to the introduction of irrational rate constant in the whole reaction system. Considering the uncertainty of the models' prediction and long last calculating time, in this study we attempt to calculate directly the collision numbers between molecules in order to interpret the discrepancy in ignition delay time measured by experiments, which can avoid the complex elementary reaction calculation involving solution of ordinary differential equation. According to the collision theory, the collision frequency between molecules is the reflection of reaction rate in essence [13]. From this point, the hard-sphere collision theory is adopted and the calculating results are compared with the experimental results.

II. EXPERIMENTS

The shock tube is 7.6 m in whole length, with a 2.5 m driver section and a 5 m driven section separated by a 0.1 m double-diaphragm section. The inner diameter is 75 mm and the wall thickness is 10 mm. Aluminum of 0.1 mm thickness is adopted and the shock tube can be operated in either single or double diaphragms if necessary. Four piezoelectric transducers (CY-YD-212, Jiangsu) are used to measure the shock velocity. Two optical windows are symmetrically located 2 cm away

*Author to whom correspondence should be addressed. E-mail: apspect@mail.tsinghua.edu.cn

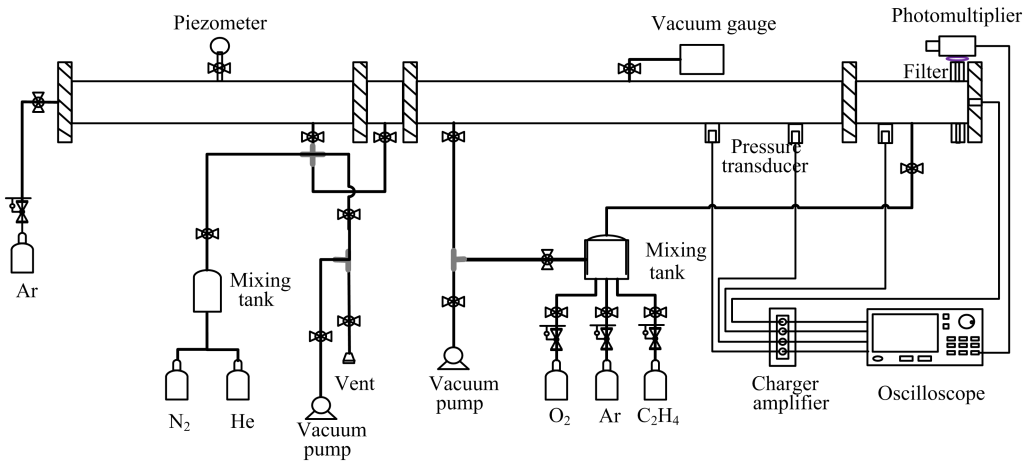

FIG. 1 Schematic diagram of shock tube apparatus.

from the endwall. The CH* chemiluminescence signal selected by a narrow filter centered at 430±5 nm (the full width at half maximum is 10 nm) is measured by a photomultiplier (PMM01, Thorlabs). All data acquisition are carried out by combination of two four-channel oscilloscopes (DSOX3024A, Agilent) triggered synchronously. Figure 1 shows schematic diagram of shock tube apparatus and only an oscilloscope is pictured.

The driver gas is composed of N_2, He, and Ar. The test time is 1.5 ms under untailored condition and can be prolonged to 8−10 ms in an approximately tailored condition if necessary.

The test gas ($C_2H_4/O_2/Ar$) is prepared in a mixing tank stewing for 24 h in accordance with the Dalton's law of partial pressure. Before each test, the driven section is vacuumized below 20 Pa and washed by the test gas 1−2 times to ensure the purity. The leakage rate is lower than 4 Pa/min. The vibrational equilibrium is considered behind both the incident and reflected shock waves and incident shock velocity is calculated by extrapolation method with an average relative uncertainty of 0.6%. Temperatures and pressures behind the reflected shock are determined using the software Gaseq [14] with an average relative uncertainty of 0.6% and 0.8%, respectively.

The ignition delay time is defined as the time interval between the arrival of the incident shock wave at the endwall and the extrapolation of the steepest rise in the sidewall CH* chemiluminescence signal to the zero baseline, as shown in Fig.2.

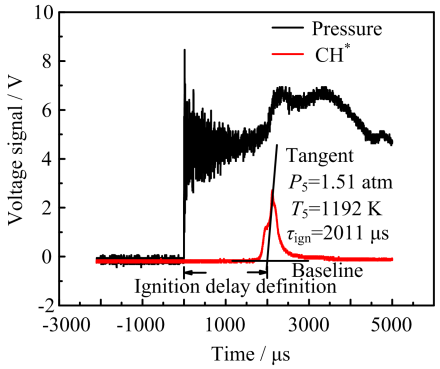

FIG. 2 Definition of ignition delay time. P_5=1.51 atm, T_5=1192 K, τ_{ign}=2011 μs.

TABLE I Experimental conditions with equivalence ratio Φ=1.

Ar diluent rate	Temperature/K	Pressure/atm
96%	1124−1743	1.3−2.7
75%	1092−1372	1.6−3.0

III. RESULTS AND DISCUSSION

A. Comparison with different ignition modes

To investigate the influence of different ignition modes on experimental results, 96% and 75% mole fractions of argon were selected with an ethylene equivalence ratio of 1. The temperature behind the reflected shock ranged from 1092 K to 1743 K, whereas the pressure ranged from 1.3 atm to 3.0 atm. The specific information can be seen in Table I.

Voevodsky *et al.* [15] first discovered two different ignition modes: strong and weak modes. Meyer *et al.* [16] proposed the partial derivative of ignition delay time *vs.* temperature to evaluate the ignition mode. Both two ignition modes have been observed in the experiments. Figure 3 is the typical pressure response of the mild ignition mode corresponding to four temperatures in 96% diluent. Both the original and the smoothing signal can be seen in Fig.3. The step signals are our goal and the high frequency vibration signal is not our interest, which

DOI:10.1063/1674-0068/29/cjcp1605104

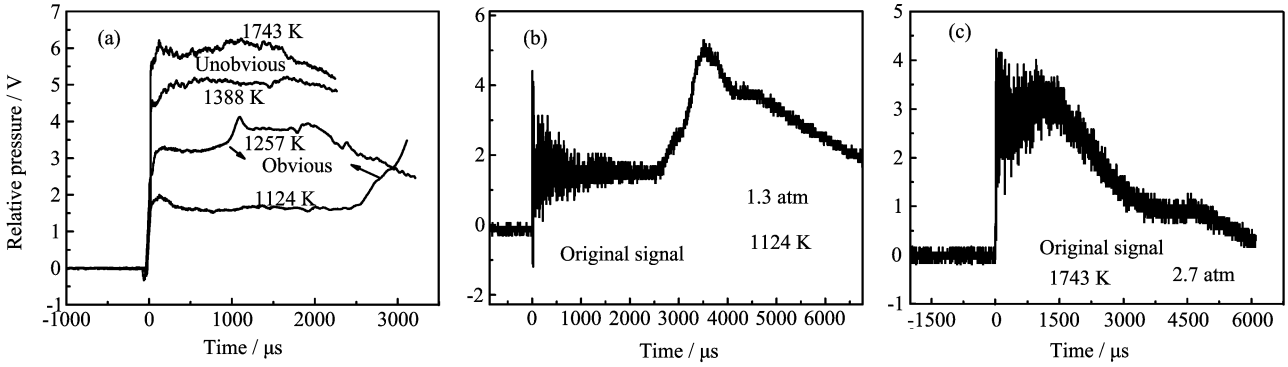

FIG. 3 (a) Pressure response of mild ignition (filtered with second order Savitzky-Golay polynomial, 96% Ar), (b) a low temperature case (1124 K), (c) a high temperature case (1743 K).

can be removed by filtering. The savitzky-golay filtering method only acts on the high frequency signal and does not work on the direct current signal. Therefore, the fidelity of the interested signal area can be assured. The first two upper curves represent a relatively high temperature and the ignition signal is not significant unless the chemiluminescence signal is added. The latter lower curve shows an obvious ignition event with a sluggish increase of pressure. It is worthy noting that this pressure rise occurs in the relative low temperature and the ignition delay is relative longer. This pressure rise is probably the result which is from the compressive wave generated by the action between reflected shock wave and the contact surface firstly, and then coupled with the reaction. The weak ignition mode attributes to the inhomogeneity of the temperature and concentration [17]. In general, the flame kernels occur in the local high temperature area, generating a series of small perturbation wave transmitting to downstream unburned area, with a feature of inconspicuous or minor increasing pressure. The so-called combustion or deflagration is the corresponding weak ignition mode.

The strong ignition mode attributes to the instantaneous combustion of huge fuel gas, generating a combustion wave to compress the unburned downstream gas, with a feature of step rise of pressure curve [17]. Figure 4(a) shows the typical pressure response of the strong ignition mode corresponding to three temperatures in 75% diluent. Likewise, both the original and the smoothing signal can be seen in Fig.4(a). Two stages can be observed. One is a sluggish rise followed by a sharp rise, whereas the other soars directly. Theoretically, ignition occurs firstly at the endwall and the pressure experiences a sluggish to sharp rise process. This is the so-called deflagration to detonation transition (DDT) process. The 1165 and 1122 K case are of this typical category. As for the 1092 K case, the pre-ignition energy release is not seen before ignition. This implies the remote ignition [18] occurs, *i.e.* the ignition occurs firstly at some distance away from the end wall, then the combustion wave spreads at the endwall. This can be verified in Fig.4(d). The sidewall pressure traces appear earlier than that of endwall.

Brown *et al.* [19] found that deflagration to detonation transition (DDT) process occurs later than obvious ignition event. Therefore, DDT has no impact upon measurement of ignition delay time. In this study, the detonation is not observed in the 96% argon diluent rate. Likewise, Kalitan *et al.* [20] did not observe the ethylene detonation under the same diluent condition.

B. Experimental analysis of ethylene ignition time correlations

In Fig.5, the experiment results are a little larger than Brown's on the whole. The two results have overlap area in the low temperature scope of the 75% diluent. The ignition delay time is extremely sensitive to temperature. Slight fluctuations in temperature because of boundary layer growth, real gas effects, shock bifurcation, *etc.* could cause a great deal of scatter. Besides, the types of ignition time definition are also an influential factor resulting in discrepancy from different experiment rigs [19]. Under both diluent conditions, the ignition delay time decreases with increased temperature. The well-fit linear relation in the logarithmic plot illustrates the ignition delay time, which fits the Arrhenius law with the reciprocal temperature. In the overlap temperature area of both diluent conditions (1092−1372 K), the ignition delay time is significantly larger under higher diluent condition at the same temperature.

As the ratio of ethylene concentration to oxygen concentration is fixed at 1:3, only one of the two species is needed. The ethylene ignition delay time correlation can be deduced through multiple linear regression analysis, as follows:

$$\tau = 3.93 \times 10^{-8}[\mathrm{C_2H_4}]^{-0.85}[\mathrm{Ar}]^{0.20} \exp \frac{E}{RT} \qquad (1)$$

where τ is the ignition delay time, $[\mathrm{C_2H_4}]$ and [Ar] are the mole concentration, E is the globe activation energy

DOI:10.1063/1674-0068/29/cjcp1605104

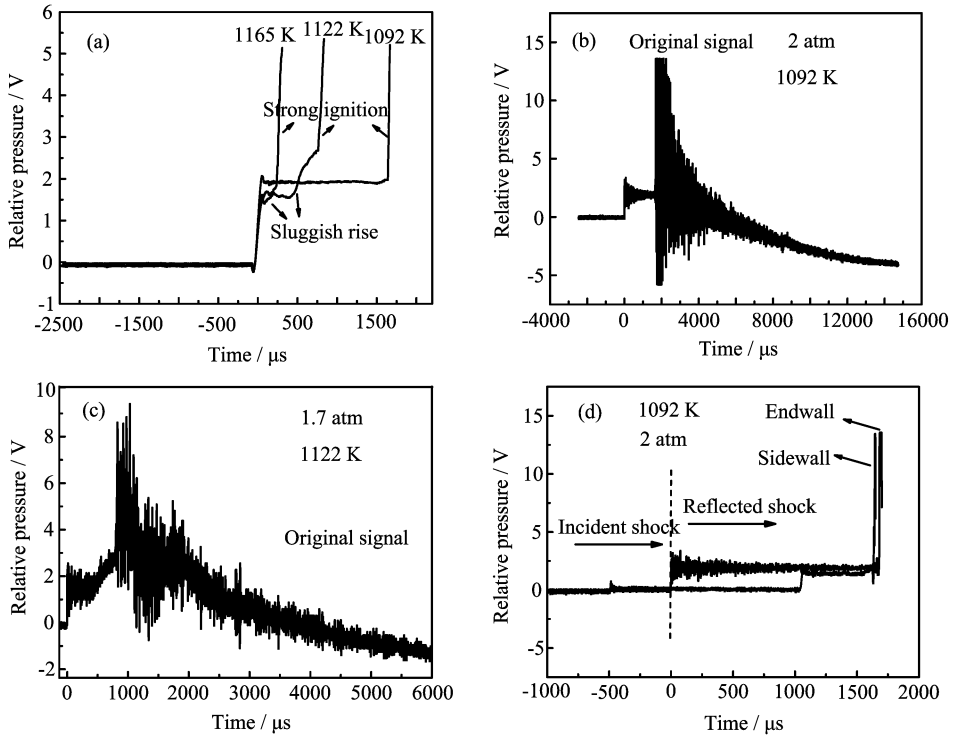

FIG. 4 (a) Pressure response of strong ignition, filtered with second order Savitzky-Golay polynomial, 75% Ar, (b) direct strong ignition, (c) deflagration to detonation transition (DDT), (d) pressure traces of remote ignition.

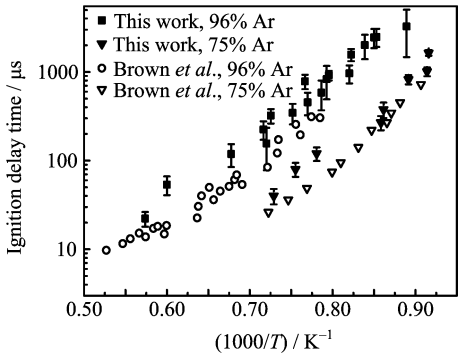

FIG. 5 Comparision of the experimrntal results in this work with Brown's results [19].

and E=31916 cal/mol, R is the universal gas constant of 1.987 cal/(mol·K), and T is the temperature.

C. Molecule collision analysis of ignition delay timeunder different diluent conditions

Eq.(1) is adopted to compare the ignition delay time under different diluent conditions. The result of the calculation shows that $\tau_{96\%}$ in 96% diluent is nearly five times larger than the $\tau_{75\%}$ in 75% diluent under the same temperature and pressure conditions.

$$\frac{\tau_{96\%}}{\tau_{75\%}} = \frac{\chi_{C_2H_4}^{1\%}\chi_{Ar}^{96\%}}{\chi_{C_2H_4}^{6.25\%}\chi_{Ar}^{75\%}} = \frac{0.01^{-0.85}\times 0.96^{0.2}}{0.0625^{-0.85}\times 0.75^{0.2}} \approx 5 \quad (2)$$

To analyze reasons for differences in ignition delay time further, the simple hard-sphere collision theory of the molecule collision theory is used. The oxygen molecule is assumed stationary and the ethylene molecule hits the oxygen molecule at an average speed of $\bar{v}$, as seen in Fig.6.

In per unit time, such a volume can be calculated as follows:

$$\Delta V = \pi(\sigma_{C_2H_4} + \sigma_{O_2})^2 \frac{\bar{v}}{4} \quad (3)$$

where $\sigma_{C_2H_4}$ and σ_{O_2} are the ethylene and oxygen molecule diameters, *i.e.*, 3.90×10^{-10} and 3.46×10^{-10} m, respectively. ΔV is the calculating area. If the molecule velocities of ethylene and oxygen obey Maxwell distribution law $f(v)$, then

$$\begin{aligned}\bar{v} &= \int_0^\infty v f(v)\mathrm{d}v \\ &= \int_0^\infty 4\pi\left(\frac{\mu}{2\pi k_B T}\right)^{3/2}\exp\left(-\frac{\mu v^2}{2k_B T}\right)v^3\mathrm{d}v \\ &= \sqrt{\frac{8k_B T}{\pi\mu}} \end{aligned} \quad (4)$$

DOI:10.1063/1674-0068/29/cjcp1605104

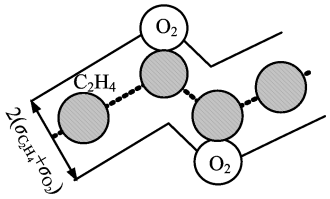

FIG. 6 Schematic diagram of molecule collision.

where k_B is the Boltzmann constant, which is 1.38×10^{-23} J/K, T is the thermodynamic temperature, μ is the reduced mass,

$$\mu = \frac{m_{C_2H_4} m_{O_2}}{m_{C_2H_4} + m_{O_2}} \tag{5}$$

where $m_{C_2H_4}$ and m_{O_2} are the ethylene and oxygen molecule mass of 4.65×10^{-26} and 5.31×10^{-26} kg, respectively.

In the volume of ΔV, all oxygen molecules would collide with ethylene molecules. If the density of the oxygen molecules n' is known, the total collision number between a single ethylene molecule with all oxygen molecules in ΔV can be calculated by the formula:

$$n_1 = n'_{O_2}\pi(\sigma_{C_2H_4} + \sigma_{O_2})^2\sqrt{\frac{8k_BT}{\pi\mu}} \tag{6}$$

$$n'_{O_2} = \frac{P_5\chi_{O_2}}{RT_5}N_A \tag{7}$$

where P_5 and T_5 are the reflected shock pressure and temperature, $\chi_{C_2H_4}$ and χ_{O_2} are the ethylene and oxygen mole fraction, and N_A is the Avogadro's number of 6.02×10^{23}.

Similarly, taking m_{Ar}=6.63×10^{-26} kg, σ_{Ar}= 3.4×10^{-10} m, the collision number n_2 between ethylene and argon and the collision number n_3 between ethylene and ethylene can be obtained. Furthermore, the probability of collision between one ethylene and all other molecules is shown below:

$$\eta = \frac{n_i}{\sum_{i=1}^{3} n_i}, \quad i = 1,2,3 \tag{8}$$

Taking the condition of 2 atm and 1500 K for an example (the average pressure in 75% diluent is 2 atm), the calculated results are as follows.

In Fig.7, the collision probability of ethylene to argon is the largest under both diluent conditions because of the increased proportion of argon, closely followed by the probability of ethylene to oxygen. The probability of ethylene to ethylene ranks the least. The collision probability of ethylene to oxygen in 75% diluent is remarkably about five times higher than that in 96% diluent.

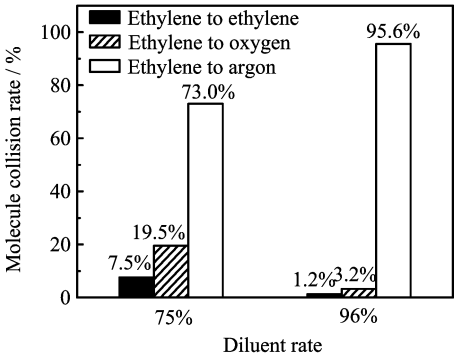

FIG. 7 Single ethylene molecule collision rate in 75% and 96% Ar diluents conditions.

Westbrook *et al.* [21] proposed a single-step overall reaction mechanism. The fuel and oxidizer concentration are adopted to reflect the overall reaction rate and the expression is

$$k_{overall} = AT^n \exp\left(\frac{-E}{RT}\right)[C_2H_4]^a[O_2]^b \tag{9}$$

Therefore, we can refer this idea and focus on the collision numbers of ethylene molecules to oxygen molecules.

Considering that the optical window is mounted 20 mm away from the endwall, a 75 mm diameter and a 2 cm height area $\Delta V'$ as the calculating object are needed to calculate the total collision number. The collision numbers by a single ethylene molecule with oxygen molecules can be obtained through Eq.(6). Hence, the total collision numbers between ethylene molecules and oxygen molecules in such an area $\Delta V'$ are given by Eq.(10), as follows:

$$n = n'_{C_2H_4}\Delta V' n'_{O_2}\pi(\sigma_{C_2H_4} + \sigma_{O_2})^2\sqrt{\frac{8k_BT}{\pi\mu}} \tag{10}$$

$$n'_{C_2H_4} = \frac{P_5\chi_{C_2H_4}}{RT_5}N_A \tag{11}$$

$$\Delta V' = \frac{1}{4}\pi d^2\Delta l \tag{12}$$

where d is the shock tube diameter, which is 75 mm, and Δl=2 cm.

Likewise, taking 2 atm and 1500 K as variable values, the final calculation results can be seen in Fig.8. The vertical axis represents (the total) collision numbers in the $\Delta V'$ area per second. The collision numbers of ethylene to oxygen are 5.99×10^{30} $s^{-1}cm^{-3}$ in 75% diluent, whereas the collision numbers are 1.53×10^{29} $s^{-1}cm^{-3}$ in 96% diluent (the black points, about 40 times the 96% results). However, the magnification of ignition delay time under two diluent conditions is just 5, which is the calculating result from Eq.(2). The discrepancy between the ignition delay time and collision numbers can attribute to steric effect [22] during molecule collision. The steric factor can be estimated by the ratio of delay

DOI:10.1063/1674-0068/29/cjcp1605104

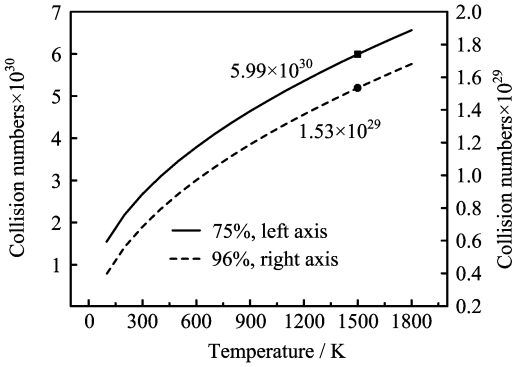

FIG. 8 Collision numbers under different temperature regions (ethylene to oxygen, 96% *vs.* 75% Ar diluent conditions).

time ratio to collision number ratio, *viz.* 5/40=0.125. Keeping the molecule density unchanged, the relationship curve of total collision numbers with temperatures can be obtained in Fig.8. The collision numbers of ethylene to oxygen increase with increased temperature under both diluent conditions. However, regardless of the temperature, the collision numbers are always about an order of magnitude higher in 75% diluent than that in 96% diluent under the same temperatures.

The increasing collision numbers enhance the chemistry reaction because collision can supply enough energy and boost the activated molecules. Hence, the ignition delay time measured in 75% diluent is dramatically reduced compared with that in 96% diluent, which is phenomeno logically confirmed in the experiments.

IV. CONCLUSION

The ignition delay time of ethylene-oxygen-argon mixture was measured in 75% and 96% diluents, respectively. The measured ignition delay time is significantly shortened in 75% diluent compared with that in 96% diluent. Meanwhile, detonation (or deflagration to detonation) phenomenon is observed in 75% diluent, whereas detonation does not occur in 96% diluent. A correlation of ignition delay time was calculated using the multiple regression method. The calculated results show that ignition delay time ratio under the two diluent conditions is nearly five. To interpret this discrepancy, the molecule collision theory is adopted. The results show that the collision numbers of ethylene to oxygen are 5.99×10^{30} $s^{-1}cm^{-3}$ in 75% diluent, whereas the collision numbers of ethylene to oxygen are 1.53×10^{29} $s^{-1}cm^{-3}$, about 40 times higher than that in 96% diluent. The discrepancy between the ignition delay time and collision numbers is the result of steric factor's influence, which can be estimated by the ratio of delay time ratio to collision number ratio, *viz.* 5/40=0.125.

V. ACKNOWLEDGMENTS

This work is supported by the National Natural Science Foundation of China (No.51676105 and No.21606143). The author would also like to thank Dr Liang Jin-hu for guiding with much useful and practical proposals.

[1] R. Brun, *High Temperature Phenomena in Shock Waves*, Springer Science & Business Media (2012).
[2] R. K. Hanson, Proc. Combustion Inst. **33**, 1 (2011).
[3] S. Wang, J. Cui, B. Fan, and Y. He, J. Chem. Phys. **18**, 897 (2005).
[4] Y. J. Zhang, Z. H. Huang, L. J. Wei, J. X. Zhang, and C. K. Law, Combust. Flame **159**, 918 (2012).
[5] S. Wang, H. Gou, B. Fan, Y. He, S. Zhang, and J. Cui, J. Chem. Phys. **20**, 48 (2007).
[6] Mechanism Downloads: http://ignis.usc.edu/USC_Mech_II.htm
[7] Mechanism Downloads: http://www.me.berkeley.edu/gri_mech/
[8] Mechanism Downloads: http://c3.nuigalway.ie/mechanisms.html
[9] T. Turányi, Reliab. Eng. Syst. Saf. **57**, 41 (1997).
[10] T. Turányi, A. S. Tomlin, *Analysis of Kinetic Reaction Mechanisms*, Berlin: Springer (2014).
[11] G. A. Pang, Proc. Combustion Inst. **32**, 181 (2009).
[12] J. Zhang, E. Hu, Z. Zhang, L. Pan, and Z. Huang, Energy Fuels **27**, 3480 (2013).
[13] Upadhyay, K. Santosh, *Chemical Kinetics and Reaction Dynamics*, Springer Science & Business Media (2007).
[14] C. Morley, *Gaseq: A Chemical Equilibrium Program for Windows*, http://www.gaseq.co.uk/
[15] V. V. Voevodsky and R. I. Soloukhin, *On the Mechanism and Explosion Limits of Hydrogen-oxygen Chain Self-ignition in Shock Waves*, Tenth Symposium (International) on Combustion, 10, 279 (1965).
[16] J. W. Meyer and A. K. Oppenheim, *On the Shock-Induced Ignition of Explosive Gase*s, Thirteenth symposium (International) on Combustion, 13, 1153 (1971).
[17] K. Fieweger, R. Blumenthal, and G. Adomeit, Combust. Flame. **109**, 599 (1997).
[18] R. K. Hanson, G. A. Pang, S. Chakraborty, W. Ren, S. Wang, and D. F. Davidson, Combust. Flame **160**, 1550 (2013).
[19] C. J. Brown and G. O. Thomas, Combust. Flame **117**, 861 (1999).
[20] D. M. Kalitan, J. M. Hall, and E. L. Petersen, J. Propul. Power **21**, 1045 (2005).
[21] C. K. Westbrook and F. L. Dryer, Combust. Sci. Technol. **27**, 31 (1981).
[22] S. R. Turns, *An Introduction to Combustion*, New York: McGraw-hill (1996).

DOI:10.1063/1674-0068/29/cjcp1605104